A Study of Boron Implantation into High Ge Content SiGe Alloys

R. Wittmann[a], S. Uppal[b], A. Hössinger[a], J. Cervenka[a], and S. Selberherr[a]

[a] Institute for Microelectronics, TU Wien, Gusshausstr. 27–29, 1040 Wien, Austria
[b] School of EE&CE, University of Newcastle upon Tyne, Newcastle NE1 7RU, UK

We report an experimental and simulation study for introducing Boron ions into high Ge content relaxed SiGe layers and into Ge wafers. The successful calibration of our Monte Carlo ion implantation simulator for this wide class of materials is demonstrated by comparing the predicted Boron profiles with SIMS data. The larger nuclear and electronic stopping power of the Ge atom is responsible for the trend to shallower profiles with increasing Ge content in SiGe alloys. The generated point defects are estimated by using a modified Kinchin-Pease model. We found that the higher displacement energy in Ge, the stronger backscattering effect, and the smaller energy transfer from the ion to the primary recoil of a collision cascade are mainly responsible for the significantly reduced damage in Ge. Finally the point responses in Si and Ge are presented and the Boron distributions are discussed.

Introduction

Scaling of Silicon MOS transistors to enhance the device performance is approaching the end in the sub-50nm regime. The gate oxide thickness cannot be scaled beyond a critical value due to the direct tunneling leakage current. Furthermore, the device lifetime is significantly reduced in ultra-thin nitrided gate oxides due to the negative bias temperature instability (NBTI) effect in p-MOSFETs. SiGe virtual substrates with high Ge contents (above 50%) or pure Germanium wafers are promising materials for high-performance CMOS applications. In recent years deep-submicron Ge-based MOS transistors with a three times mobility improvement in comparison to Silicon devices were processed using an HfO_2 based high-k dielectric on 200mm Ge wafers by using a Silicon-like process flow (1,2). The junction leakage current is about four decades higher for Ge than for Si at a chip temperature of 110°C. The reduction of the extremely high leakage current will therefore be a key issue for Ge-based CMOS technology to obtain devices with reasonably low I_{off} current. Ge rich $Si_{1-x}Ge_x$ alloys ($x > 80\%$) and pure Ge have been recognized as promising materials for photodetectors in optical transmission systems due to the high optical absorption coefficient for an operation at a wavelength of $1.3\mu m$ in the near infrared (NIR) regime (3,4). The use of epitaxial Ge-on-Si technology allows the integration of interdigitated Ge pin-photodiodes with CMOS circuits on a Silicon chip to build optical communication receivers with low fabrication costs. Optical chip-to-chip communication solutions and/or optical on-chip interconnects are required in order to meet the challenges of differentiated, high-performance systems in the near future.

While ion-implanted dopant profiles are well studied in Silicon for various dopant species and implantation conditions, dopant profiles are scarce in SiGe alloys as well as in pure Ge. However, an accurate and multi-dimensional simulation of ion implantation processes is required for these target materials to optimize the doping profiles for CMOS applications and for integrated optoelectronic devices. We present the results of our experimental and simulation study for introducing Boron ions into crystalline SiGe and Ge with energies in the range from 5 to 20keV. All simulations were performed with our Monte Carlo implantation simulator MCIMPL-II (5,6). The measured Boron profiles were used to extend the simulator to SiGe alloys with Ge content from 50% up to pure Ge. The calibrated simulator is able to accurately predict the as-implanted Boron profiles and to estimate the produced point defects.

Simulation Method

The multi-dimensional ion implantation simulator MCIMPL-II is based on a BCA method and uses the universal ZBL potential (7). Lattice vibrations are considered by the Debye model with a Debye temperature of 450K. An empirical electronic stopping model (8) is applied and the damage accumulation is calculated by the modified Kinchin-Pease model (9) together with a model for point defect recombination. The simulator can handle complex three-dimensional device structures consisting of various amorphous materials and crystalline Silicon.

Si and Ge, which both crystallize in the diamond lattice structure, are completely miscible forming $Si_{1-x}Ge_x$ solids with x ranging from 0 to 1. We extended the target materials of the simulator from crystalline Silicon to the class of $Si_{1-x}Ge_x$ alloys and Ge by adjusting the lattice parameter $a(x)$ of the crystalline model as a function of the Ge fraction x according to

$$a(x) = 0.02733\ x^2 + 0.1992\ x + 5.431 \quad (\text{Å}) \tag{1}$$

which approximates experimental data with a maximum deviation of about 10^{-3}Å (10). While the ion moves through the simulation domain, a local crystal model (as shown in Fig. 1) is built up around the actual ion position for searching the next collision partner. The selection of the target atom species for $Si_{1-x}Ge_x$ alloys is defined by probability x for Ge and $(1-x)$ for Si, respectively. In a screened Coulomb collision the energy loss of the ion, ΔE, is equal to the transferred energy to the recoil atom,

$$\Delta E = \frac{4\,M_1\,M_2}{(M_1 + M_2)^2} \cdot \sin^2\frac{\Theta}{2} \cdot E_0 \tag{2}$$

where M_1 and M_2 are the masses of ion and target atom, Θ is the transformed scattering angle in the center-of-mass coordinates, and E_0 is the kinetic energy of the ion before the collision event (11). From this equation it can be derived that a smaller energy loss ΔE occurs in nuclear collisions in Ge targets due to the different masses between ion and atom. The transferred energy ΔE from a Boron ion to a Ge atom is
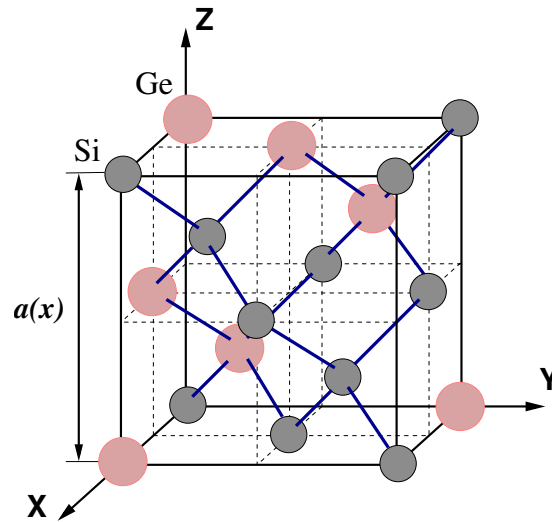
Fig. 1: Local crystal model used for the simulation of Si, $Si_{1-x}Ge_x$ alloys of arbitrary Ge content, and Ge ($0 \leq x \leq 1$).

approximately the half (0.568-fold) compared to ΔE in Si at a given scattering angle. Note that the difference in masses between Boron and Ge leads also to a stronger backscattering effect which produces shallower profiles.

The modified Kinchin-Pease model assumes that the number of displaced atoms (Frenkel pairs) in a recoil cascade is a function of the transferred energy ΔE from the ion to the primary recoil atom. However, a critical parameter for the produced damage is the threshold displacement energy required for the incoming ion to displace a target atom. A displacement energy E_d of 15eV has become widely accepted for the well-known Silicon. We fitted a value of $E_d = 30$eV for Ge by comparing simulated Boron profiles with SIMS data. The larger E_d value is responsible for producing significantly lesser point defects by Boron ions in Ge than in Si at a given recoil energy. The used value for the displacement energy is in good agreement with $E_d = 31$eV which was deduced for Ge in (12). Fig. 2 compares the number of produced point defects for a damage cascade in Si and Ge, calculated by the modified Kinchin-Pease model.

We calibrated the Lindhard correction parameter k_L of the empirical electronic stopping model to adopt the strength of the electronic stopping process which increases with the Ge content in the alloy (13). We used the parameter $k_L = 1.75$ for Si and a value of 1.9 for Ge.

The Monte Carlo method is based on computing a large number of individual ion trajectories in the simulation domain by using appropriately scaled random numbers. After performing the Monte Carlo calculation, the dopant and damage data are both stored in histogram cells aligned on an orthogonal grid. The Monte Carlo result is
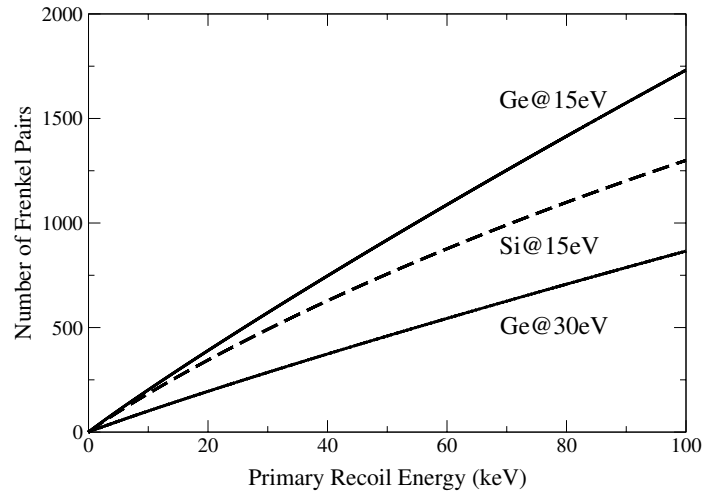
Fig. 2: Number of Frenkel pairs generated by a primary knock-on atom in Si assuming $E_d = 15\text{eV}$, and in Ge assuming $E_d = 15\text{eV}$ or 30eV.

then smoothed and translated from the internal orthogonal grid to an unstructured destination grid suitable for the subsequent simulation of annealing processes. We performed the simulation of one-dimensional profiles with at least 10^6 trajectories.

Experimental Details

Relaxed SiGe layers were grown on (100) Silicon substrates using Low Energy Plasma Enhanced Chemical Vapor Deposition (LEPECVD). A grading technique was applied (7% per micron) to obtain the desired Ge composition of (53, 63 or 86%). Following this deposition a constant composition layer with a thickness of about 1μm was finally grown which is implanted with Boron ions. (100) oriented Ge wafers were also implanted at the same implantation conditions. Secondary Ion Mass Spectroscopy (SIMS) was used to measure the implant profiles. Some of the strongly noisy SIMS data are smoothed with a Bernstein polynomial approximation (14) to better see the trend of the measured profile.

Results and Discussion

Ge has a larger nuclear and electronic stopping power for ion-implanted dopants due to the heavier and electron-rich atomic structure. Therefore the projected range of an implanted dopant profile in Ge is shallower than in Si for any given energy. Fig. 3 compares the Monte Carlo results performed with our calibrated ion implantation simulator to SIMS measurements. The pre-amorphization was performed by an
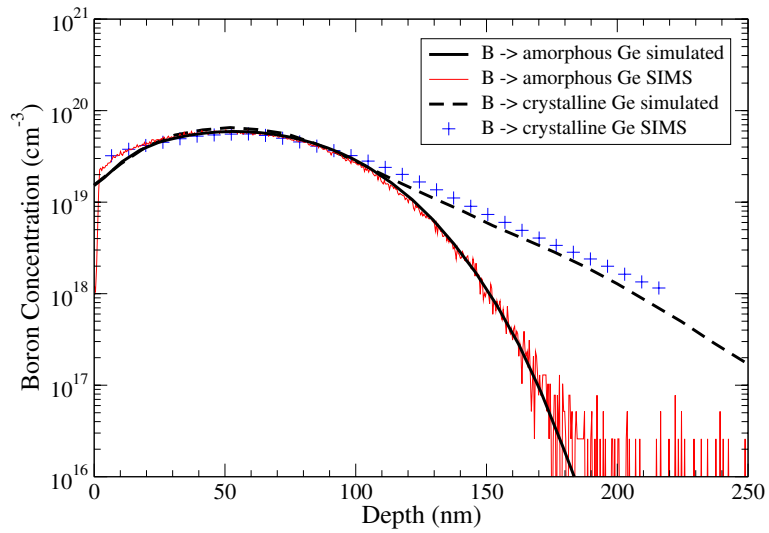
Fig. 3: Simulated 20keV Boron implants in amorphous Ge and in (100) Ge using a dose of $6 \cdot 10^{14} \text{cm}^{-2}$ and a tilt of $7°$ compared to SIMS data.
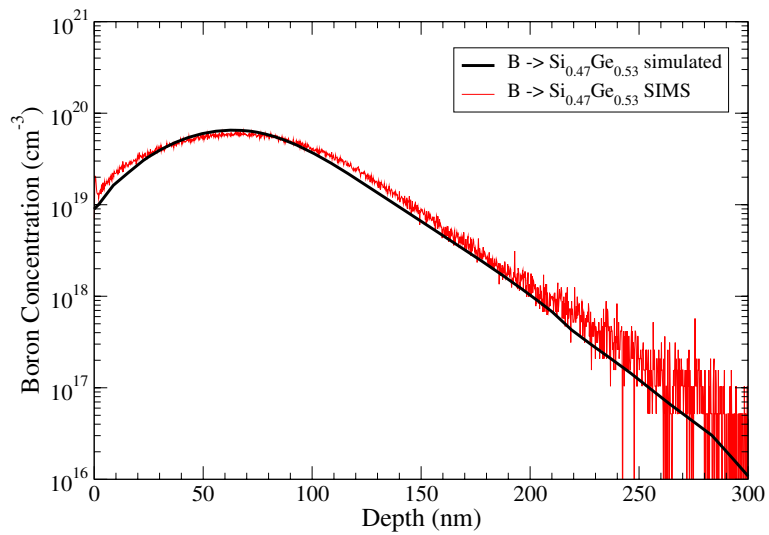

Fig. 4: Simulated 20keV Boron profile in (100) $Si_{0.47}Ge_{0.53}$ using a dose of $6 \cdot 10^{14} \text{cm}^{-2}$, and a tilt of $7°$ compared to SIMS.
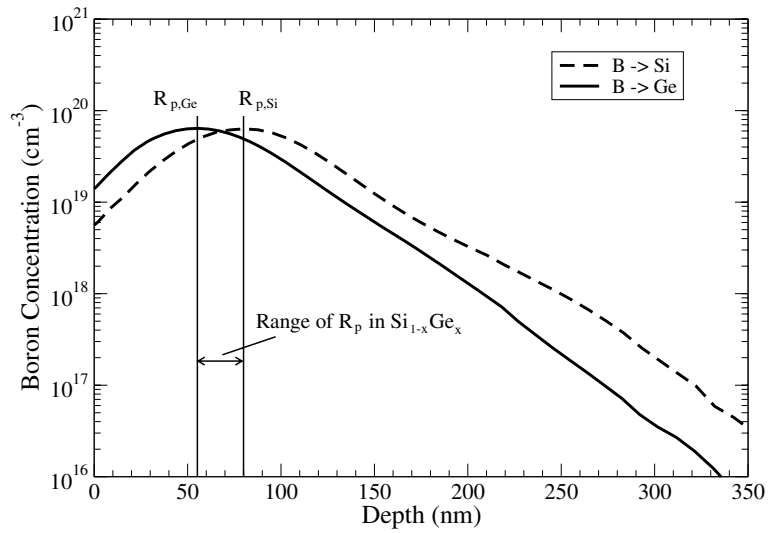
Fig. 5: Comparison of simulated 20keV Boron implants in Si and Ge using a dose of $6 \cdot 10^{14} \mathrm{cm}^{-2}$ and a tilt of $7°$.
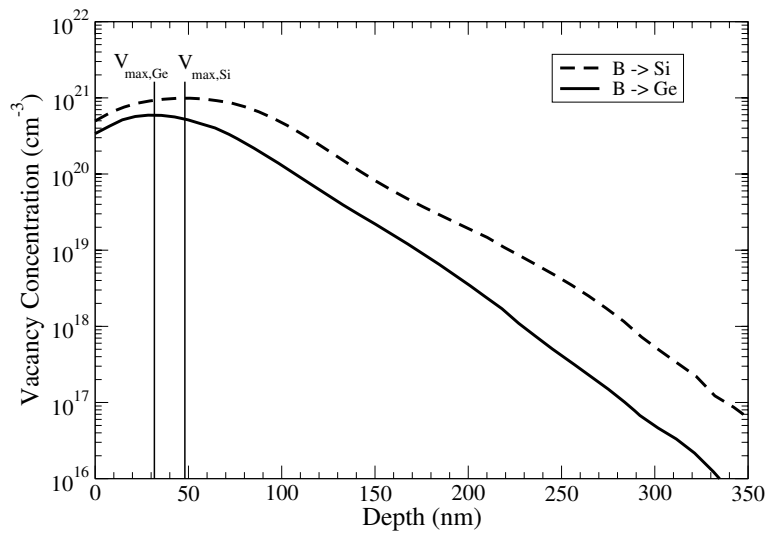

Fig. 6: Comparison of produced vacancies for 20keV Boron implantation in Si and Ge using a dose of $6 \cdot 10^{14} \mathrm{cm}^{-2}$ and a tilt of $7°$.

implantation of ^{72}Ge with an energy of 200keV and a dose of 10^{15}cm^{-2}. The Boron implantations into amorphous Ge and into crystalline Ge were performed with an energy of 20keV, a dose of $6 \cdot 10^{14}$cm^{-2}, and a tilt of 7°.

In former work we confirmed a non-linear shift towards shallower profiles with increasing Ge content for low Ge content Si$_{1-x}$Ge$_x$ alloys (x $\leq$ 0.5) (13). The as-implanted Boron profiles in SiGe layers with 53%, 63%, and 86% Ge content are very similar. Fig. 4 compares the simulation result for a 20keV Boron implantation into crystalline Si$_{0.47}$Ge$_{0.53}$ using the same implantation conditions as in Ge. We found the projected range R_p of the Boron distribution in Si$_{0.47}$Ge$_{0.53}$ at a depth of 65nm which is well within the projected ranges for Ge (55nm) and Si (80nm) using the same conditions. Fig. 5 demonstrates that the larger nuclear and electronic stopping power of Ge produces a significantly shallower profile as well as a slightly reduced channeling effect in the tail region. An advantage of the Monte Carlo simulation is that the used Kinchin-Pease damage model allows to estimate the produced vacancies in the crystal. Note that equal local concentrations of vacancies and interstitials are assumed, since the recoils themselves are not individually followed in our computationally fast simulation approach. Fig. 6 compares the simulated vacancy concentration profiles in Si and Ge which are associated with the Boron implants presented in Fig. 5. The maximum of the vacancy concentration lies close to the middle between the wafer surface and the projected range in both cases. The maximum is not at the surface since the electronic stopping process dominates at the high initial energy of the ions, when they enter the crystal. In other words, the Boron ions enter most likely a channel at the surface and despite of their tilted incident direction they can stay at least a short distance inside a channel. The used higher displacement energy of 30eV, the stronger backscattering mechanism for Boron ions in Ge as well as the smaller energy transfer ΔE from the ion to the primary recoil of a cascade are mainly responsible for the significantly smaller damage production in Ge. This is consistent with the experimental observations in (15) that 100% of the implanted Boron ions in Ge are immediately active without annealing for using a relatively high dose of 10^{14}cm^{-2} and for energies ranging from 25–150keV, since Boron implanted Ge remains crystalline.

Table 1 summarizes simulated and measured R_p and σ_p parameters for Boron implants in crystalline Si, Si$_{0.5}$Ge$_{0.5}$, and Ge targets. The projected range R_p is read off at the maximum concentration of implanted Boron ions and the provided straggling σ_p is the mean value of the left and right straggling values which are determined by 60% of the maximum Boron concentration. All simulations were performed with a dose of 10^{14}cm^{-2} and a tilt of 7°.

Material	Si	Si$_{0.5}$Ge$_{0.5}$	Ge	Si	Si$_{0.5}$Ge$_{0.5}$	Ge
Energy (keV)	5	5	5	20	20	20
R_p (nm)	18.91	15.44	14.32	79.52	65.32	55.27
σ_p (nm)	14.16	12.56	12.16	37.42	36.33	39.38
SIMS R_p (nm)	-	-	16.23	-	67.11	56.99
SIMS σ_p (nm)	-	-	11.23	-	40.58	34.91

Table 1: Simulated and measured parameters for projected range and straggling.
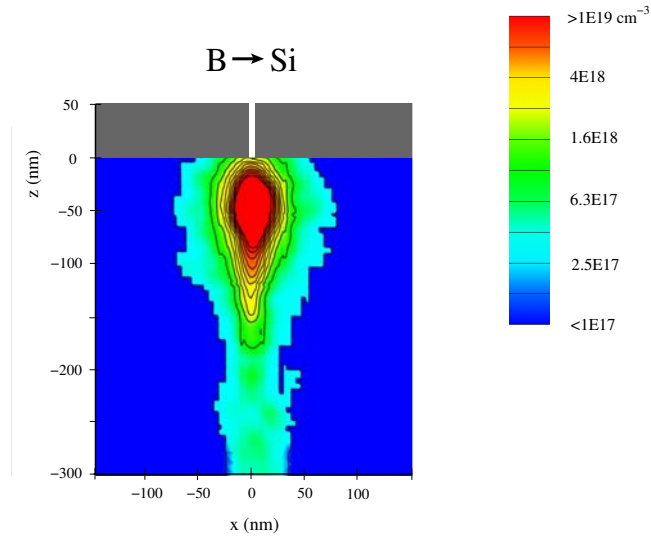
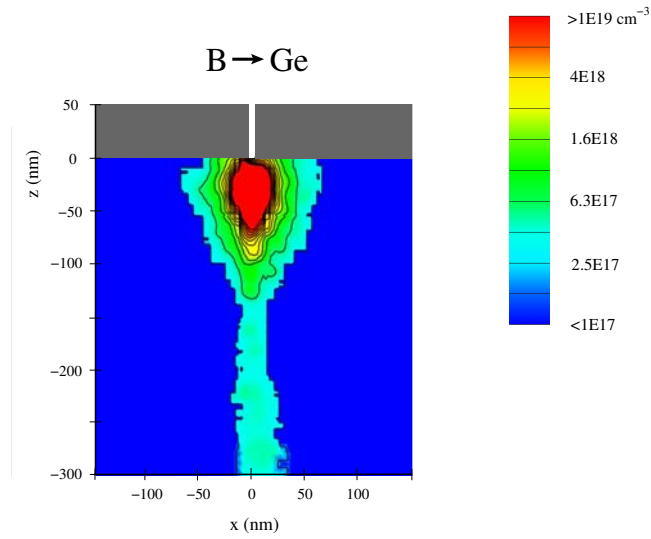Fig. 7: Simulated point response for a 10keV high-dose implantation of Boron into crystalline Silicon.

Fig. 8: Simulated point response for a 10keV high-dose implantation of Boron into crystalline Germanium.

The point responses in crystalline Si and Ge are compared in Fig. 7 and Fig. 8. The width of the implantation window in an impenetrable mask is 8nm. Boron is implanted with an energy of 10keV, a dose of $5 \cdot 10^{15} \text{cm}^{-2}$, and the ion beam is 7° tilted in such a way that the lateral component of the incident direction is parallel to the direction of view ($< 010 >$ direction). Therefore the presented point responses appear symmetric. Approximately 420000 simulated ion trajectories enter the substrate and contribute to the Boron distribution. While the lateral penetration depth of Boron ions is only slightly reduced, the vertical depth is strongly reduced in Ge. The channeling tail is closely centered around the <100> axis in both cases. This demonstrates that in (100) Si or Ge, axial channeling in the <100> direction dominates by far over channeling in other directions.

Conclusion

Boron implantation in high Ge content SiGe alloys (Ge content $\geq 50\%$) and in pure Ge has been studied using SIMS measurements and a physics-based simulation approach. We showed that the calibrated Monte Carlo ion implantation simulator can accurately predict the Boron profiles for different energies and doses. The simulator can estimate the produced vacancies in the crystal, which are associated with a specific Boron implantation profile. We found that the damage accumulation in Ge is significantly reduced compared to Si, which is consistent with former experimental observations indicating that Boron implanted Ge remains essentially crystalline. The simulated point responses revealed that the Boron distribution is significantly reduced in Ge in the vertical direction, while the lateral profile is quite similar in Si and Ge.

Acknowledgments

References

1. A. Delabie, R. L. Puurunen, B. Brijs, M. Caymax, T. Conard AND B. Onsia, O. Richard, W. Vandervorst, C. Zhao, M. M. Heyns, M. Meuris, M. M. Viitanen, H. H. Brongersma, M. Ridder, L. V. Goncharova, E. Garfunkel, T. Gustafsson, and W. Tsai, *J. Appl. Phys.*, **97**(6), p. 1 (2005).
2. M. Meuris, B.De Jaeger, S. Kubicek, P. Verheyen, J.Van Steenbergen, G. Lujan, E. Kunnen, E. Sleeckx, I. Teerlinck, S.Van Elshocht, A. Delabie, R. Lindsay, A. Satta, T. Schram, T. Chiarella, R. Degraeve, O. Richard, T. Conrad, J. Poortmans, G. Winderickx, M. Houssa, W. Boullart, M. Schaekers, P.W. Mertens, M. Caymax, S.De Gendt, W. Vandervorst, E.Van Moorhem, S. Biesemans, K.De Meyer, L. Ragnarsson, S. Lee, G. Kota, G. Raskin, P. Mijlemans, V. Afanas'ev,

A. Stesmans, and M. Heyns, in *SiGe: Materials, Processing, and Devices*, PV 2004-07, p. 693 ECS, Pennington, NJ (2004).

3. R. E. Jones, S. G. Thomas, S. Bharatan, R. Thoma, C. Jasper, T. Zirkle, N. V. Edwards, R. Liu, X. D. Wang, Q. Xie, C. Rosenblad, J. Ramm, G. Isella, H.von Känel, J. Oh, and J. C. Campbell, in *Proc. Int. Elec. Dev. Meet. (IEDM)*, p. 793 (2002).

4. L. Colace, M. Balbi, G. Masini, G. Assanto, H. C. Luan, and L. C. Kimerling, *J. Appl. Phys. Lett.*, **88**(10), (2006).

5. G. Hobler and S. Selberherr, *IEEE Transactions on CAD*, **8**(5), 450 (1989).

6. R. Wittmann, A. Hössinger, and S. Selberherr, in *Proc. 15th European Simulation Symposium (ESS 2003)*, A. Verbraeck and V. Hlupic, Editors, p. 35, Delft (2003).

7. J. Ziegler, J. P. Biersack, and U. Littmark, *The Stopping and Range of Ions in Solids*, p. 41, Pergamon Press, Oxford (1985).

8. G. Hobler, A. Simionescu, L. Palmetshofer, C. Tian, and G. Stingeder, *J. Appl. Phys.*, **77**(8), p. 3697, (1995).

9. M. J. Norgett, M. T. Robinson, and I. M. Torrens, *Proc. Nuc. Eng. Des*, **33**, p. 50 (1975).

10. E. Kasper and K. Lyutovich, *Properties of Silicon Germanium and SiGe:Carbon*, p. 47, Inspec, London (2000).

11. J. Ziegler, *Ion Implantation Science and Technology*, p. 207, Ion Implantation Technology Co., New York (1996).

12. E. W. J. Mitchell *Br. J. Appl. Phys.*, **8**, p. 179 (1957).

13. R. Wittmann, A. Hössinger, and S. Selberherr, in *SiGe: Materials, Processing, and Devices*, PV 2004-07, p. 181 ECS, Pennington, NJ (2004).

14. C. Heitzinger and S. Selberherr, *Proc. Simulation of Semiconductor Processes and Devices (SISPAD)*, p. 420 (2001).

15. K. S. Jones and E. E. Haller *J. Appl. Phys.*, **61**(7), p. 2469 (1987).